

Effect of Ar⁺ and H⁺ etching on the magnetic properties of Co/CoO core-shell nanoparticles

P. Imperia, D. Schmitz, and H. Maletta

Hahn Meitner Institut, Glienicker Strasse 100, 14109 Berlin, Germany

N. S. Sobal and M. Giersig

CESAR Research Center, Department of Nanoparticle Technology, Ludwig-Erhard-Allee 2, 53175 Bonn, Germany

(Received 1 December 2004; published 19 July 2005)

The *ex situ* preparation of chemically synthesized cobalt nanoparticles leads unavoidably to particles coated with organic surfactants and a thin CoO shell. Argon ion (Ar⁺) etching is a method often used to remove the surfactant and the oxide shell. *Ex situ* prepared nanoparticles of 9.7 nm diameters were investigated as a function of the sputtering time, by means of soft x-ray absorption spectroscopy at the C and O K edges and at the Co L_{2,3} edges. Low-energy (500 eV) Ar⁺ ion etching was effective in removing the organic coating layer of the nanoparticles, while much higher energy and longer sputtering times were required to affect the CoO shell. On the other hand, only a short time using low-energy hydrogen ion (H⁺) etching was necessary to completely reduce the oxide shell. Magnetic circular dichroism of soft x-rays was used to measure the magnetic properties of the etched samples. We found that the orbital to spin magnetic moment ratio, μ_l/μ_s^{eff} , increases as a function of the Ar⁺ etching time. Such an increase may be ascribed to the incomplete removal of the CoO shell as well as to surface strain, increased roughness, and an effective reduction of the particle size induced by the high-energy ion etching. A much smaller effect was observed for the low-energy (500 eV) and short time H⁺ etched samples, where the magnetic moment ratio after the reducing procedure $\mu_l/\mu_s^{\text{eff}}=0.12$ is comparable to values obtained for bulk cobalt.

DOI: [10.1103/PhysRevB.72.014448](https://doi.org/10.1103/PhysRevB.72.014448)

PACS number(s): 75.75.+a, 78.70.Dm, 81.40.Rs

I. INTRODUCTION

To cast a colloidal solution of nanoparticles (NPs) on a Si substrate represents an easy, fast, and cost-effective way to prepare regular two-dimensional arrays of self-assembled NPs. Several well-established chemical routes have been devised to prepare dispersions of Co particles on a mesoscopic scale. Slightly different chemical synthetic paths allow the preparation of NPs with distinct crystallographic characteristics: it is possible to prepare NPs having the hexagonal close packed (hcp), or the face-centered cubic (fcc)¹ crystal structures. It was also observed that a metastable cubic crystal structure, so called ϵ -Co, is accessible for Co powders prepared through the chemical synthetic route.^{2,3} A toluene based dispersion of NPs obtained by chemical synthesis can be deposited on the substrate of choice to produce samples of self-assembled, well-separated metallic crystals.

High resolution transmission electron microscopy (HR-TEM) measurements show that samples prepared in this way contain particles of a regular spherical shape possessing a sharp size distribution.⁴ The crucial point for the chosen sample preparation technique is the ability to easily tailor and strictly control the particle diameters. Such an ability allows, in principle, the fine tuning of the final magnetic properties of the samples by engineering their anisotropy.

The size of the NPs plays an important role and for particles on a nanometer scale peculiar physical and chemical properties are reported. Studies of Fe clusters, for example, show that both the orbital (μ_l) and the spin (μ_s^{eff}) magnetic moments increase by decreasing the cluster size, and the orbital to spin magnetic moment ratio μ_l/μ_s^{eff} exceeds many times the bulk value.⁵

The presence of oxide on the surface of metallic NPs prepared *ex situ* by chemical synthesis is unavoidable. However, because of the oxidation occurring only in the first layers of the particles, we can also regard them as a truly core-shell ferromagnetic-antiferromagnetic (FM/AF) “ready to use” system. They therefore could have interesting technological applications for example in spintronics.⁶ Previous works on colloidal solutions of Ar⁺ ion etched NPs found that the Co/CoO interface plays a crucial role in a dramatically enhanced μ_l/μ_s^{eff} ratio.⁷ On the other hand, according to ferromagnetic resonance (FMR) measurements, NPs that have not been Ar⁺ ion etched show no enhanced μ_l/μ_s^{eff} ratio, resulting in a value of the spin to orbital magnetic moment ratio corresponding to that of bulk Co.⁷

Several factors play a role in their contrasting results: first, as FMR is sensitive to the whole FM core of NPs it is not strongly influenced by the AF CoO layer. On the other hand, magnetic circular x-ray dichroism (XMCD) shows an enhanced μ_l/μ_s^{eff} ratio. As the absorption spectra, measured recording the electron yield, are sensitive primarily to the magnetic properties of the surface and near-surface interfaces of the system, the role of surface effects are crucial. Moreover, the NPs surface is especially complex and cannot be easily defined, since the NPs are covered with layers of a mixture of CoO and Co₃O₄,⁸ and a mixture of organic surfactants and residuals of the chemical synthesis. The full nature of the discrepancy between the XMCD measurements and the FMR results, as well as the unanswered questions connected with the NPs surface properties need to be clarified. Thus motivated we have undertaken a careful investigation of the effect of Ar⁺ and H⁺ ion etching on the surface and the magnetic properties of such *ex situ* chemically synthesized nanodimensional crystals.

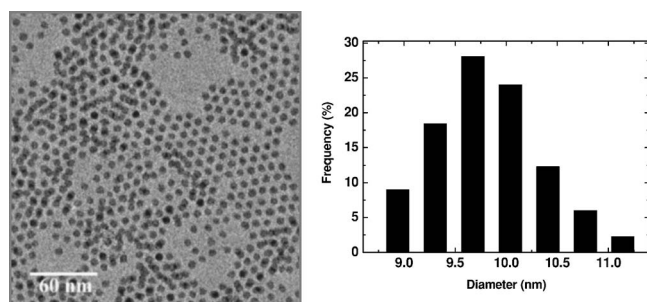


FIG. 1. TEM image and size distribution of Co (fcc) nanoparticles.

X-ray absorption spectroscopy (XAS) is a method that enables one to discriminate between surface, interface, and bulk properties. It has surface and near-surface sensitivity, element specificity, and it is well suitable for the study of interfaces.⁹ The application of the sum rules in the analysis of the XMCD measurements links the measured spectra to the value of the spin and orbital moment per atom and their anisotropy. The separation and determination of atomic spin and orbital moments are the key abilities enabled by the experimental technique that become extremely useful in this kind of comparative studies.

II. EXPERIMENTAL

The Co/CoO core/shell NPs were prepared following the well-established synthetic route described in Ref. 1. To attain a solution of NPs of mainly the same size the particles were prepared by thermal decomposition of dicobaltotocarbonyl [Co₂(CO)₈] in the presence of stabilising ligands, and size-selective precipitation was used twice in order to narrow the size distribution of the nanocrystals. The resulting colloidal solution was then deposited on a chemically cleaned Si surface. The solvent was evaporated at a controlled rate and the final result was a film of regularly spaced particles of 9.7 nm diameter having a very narrow size distribution with a standard deviation of about 5% (Fig. 1). The NPs prepared according to the above described technique are covered with an organic surfactant, which is oleic acid¹⁰ and with a native shell of CoO of some monolayer thickness. The arrays of Co NPs were further characterized by superconducting quantum interference device (SQUID) magnetometry. The magnetometric measurements show that the NPs “as prepared” possess a remanent field of about 8.7 KG at 15 K. No remanent field was found at temperatures higher than 70 K.

The samples were studied in a ultrahigh vacuum (UHV) chamber after *in situ* Ar⁺ or H⁺ ion etching by means of an ion gun (10/35 SPECS). The surface-sensitive and material selective XAS technique allowed us to investigate the progress of the sample properties after each etching step. We examined the L_{2,3} edges of Co and the K edges of O and C, measuring the total electron yield by means of the sample drain current. The magnetic properties of the etched samples were studied by XMCD, i.e., by subtracting two subsequent XAS energy spectra recorded with opposite circular polarization or opposite magnetization direction. The measurements

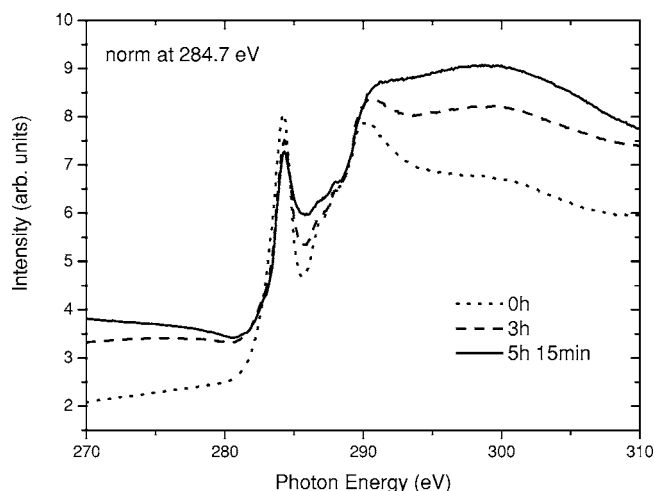


FIG. 2. Co nanoparticles (7.7 nm) at C K edges under x-ray illumination. The spectra are normalized at 284.7 eV and with a cleaned Si substrate.

were performed at the beamline UE46 PGM at the synchrotron radiation facility BESSY (Berlin), which allows switching between different polarization modes: circular and linear polarization under various angles. The beam line is characterized by a very high photon flux with a typical value of 10¹² photons/s, 0.1 Å in the energy range of interest.¹¹ The XMCD signal was measured by reversing the photon helicity (indicated as σ^+ and σ^- for the remainder of the paper) of two successive energy scans of the circularly polarized incoming beam in the case of the Ar⁺ etched samples or reversing the magnetic applied field in the case of the H⁺ etched ones. The energy resolution of the beamline monochromator during the XAS spectra was better than 0.2 eV. The base pressure in the UHV chamber during the measurements was better than 4×10^{-10} mbar. The XMCD spectra were recorded in grazing incidence at an angle of 20° with respect to the substrate plane. All the curves were normalized for the synchrotron intensity fluctuation and beamline transmission coefficients by means of the last mirror current.

III. RESULTS AND DISCUSSION

When starting the XAS experiment at BESSY the question arose immediately about the stability of the NPs sample under the high photon flux of the beam. We observed that under illumination of the synchrotron radiation the spectra taken at the Co L_{2,3} absorption edges exhibited an unusual rising background with time. The increase was nearly linear during the first hour of measurement, then it turned slowly to saturation and remained stable after a few more hours of illumination. While at the Co L_{2,3} edges this effect influenced only the background of the spectral curves without any change of their shape, this scenario did not hold for the K edge of C. The spectra in Fig. 2, taken with NPs of 7.7 nm diameter, clearly show how the shape of the C K edge typically changes over time. The peak at about 290 eV tends to disappear under a much broader feature at around 300 eV that strongly increases in intensity over time. The main peak

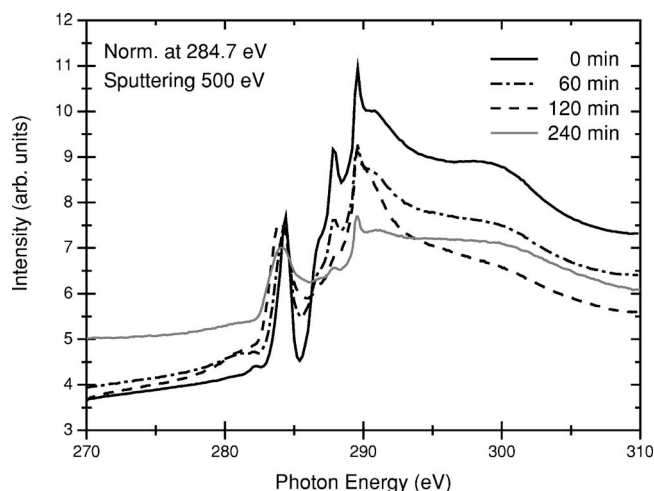


FIG. 3. Co nanoparticles (9.7 nm) at C K edges at an increasing Ar⁺ etching time (500 eV). The spectra are normalized at 284.7 eV and with a cleaned Si substrate.

at 284.4 eV, the typical main $1s$ line for many compounds containing C, remains substantially unaltered in shape and weight during the observing time. The background rise effect was observed only during the first exposition of the NPs to synchrotron radiation. For this reason we can reasonably exclude the possibility that the effect was caused by a charging of the samples. The background rise as function of the soft x-ray exposition time was not observed for sputtered samples and so we may assume that under the intense synchrotron light beam it is the NPs organic coating material that gets damaged.

A. Ar⁺ etching

Figure 3 shows the evolution of the spectra near the C K edge at different sputtering times. Ar⁺ ion etching with moderate energy, 500 eV kinetic energy, modifies the organic coating, while at the Co L_{2,3} edges no significant differences are recorded. After 240 min of sputtering at the same energy there is no further evolution of the spectrum near the C K edge. With further sputtering it remains unchanged, while the spectrum at the Co L_{2,3} edges starts to be strongly affected. This finding provides for a direct confirmation that Ar⁺ ion etching of a moderate energy (500 eV) can remove the organic coating layer without substantially affecting the CoO shell, however, traces of C are still present also after a longer sputtering time. In Fig. 4 the first obtained spectrum, labeled with time 0, shows the Co L_{2,3} absorption edges as the sample is introduced in the UHV chamber. The presence of CoO on the surface of the NPs can immediately be recognized by the typical splitting of the main peak. The spectra show the typical CoO complex structure dominated by three main peaks at the Co L₃ edge and two further peaks of minor intensity. As expected, the L₂ edge does not show any splitting, considering its typical lifetime broadening. After 120 min of etching at 500 eV, there are no substantial changes, i.e., the two peaks at 775.6 and 776 eV are still present, while the minor side peak at 776.6 eV is reduced to a shoulder, however, the CoO character still remains. After

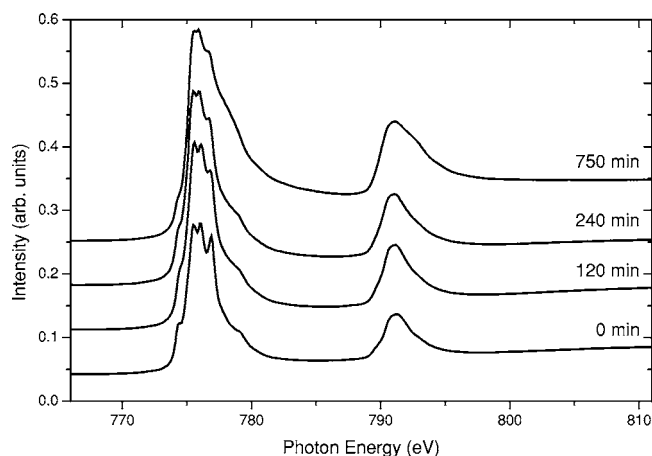


FIG. 4. Nanoparticles (9.7 nm) at Co L_{2,3} edges at increasing Ar⁺ etching time (500 eV, last 350 minutes at 900 eV). A vertical offset is used for clarity.

240 min of sputtering, the typical multiplet structure of CoO is less defined. By only increasing the sputtering energy to 900 eV and etching for a further 350 min at this higher energy, however, it is possible to finally start to observe the metallic Co single peak at 775.7 eV accompanied by a broadening of the Co L₂ absorption edge spectrum, while the shoulder at 776.6 eV remains substantially unaffected.

A considerable change in the lineshape of the O K edge was recorded only after 450 min of sputtering at 500 eV followed by a further 270 min at a higher energy (900 eV). This major alteration in the lineshape indicates that the O edge evolves under the effect of the Ar⁺ ions and this shape variation definitely coexists with the lineshape changes registered at the Co L₃ edge.

After the soft Ar⁺ sputtering at 500 eV for 240 min and a further 350 min at 900 eV, the sample was cooled to 15 K and magnetized with a pulsed field of about 0.4 T produced by conventional coils at constant temporal intervals during the cooling. Despite the increased metallic character of the XAS spectra with respect to the nonetched samples, no magnetic dichroism was observed. Only after further etching at much higher energies a dichroic signal appeared. The spectra observed at the O K edge confirmed the view of an untouched CoO shell at low-energy sputtering. Figure 5 shows how the O K edge of the samples evolved during etching: At low-energy Ar⁺ sputtering, no major changes were recorded, the O K edge remained unchanged until the sputtering energy was increased. From our observations we can conclude that only at high energy can the sputtering with Ar⁺ be effective in removing the CoO layer; both the Co edges and the O edge show significant changes only after at least 250 min of ions etching, when the shape of the C white line was not affected anymore, which becomes obvious comparing Figs. 3, 4, and 5.

XAS spectra taken of nonetched samples at the O K edge, and compared to the reference compounds of CoO and Co₃O₄ in NPs and thin layers,⁸ confirm that the surface of the nanoparticles, as suspected, is covered from the beginning, with a shell composed of a mixture of the two forms of the metal oxide, being the spectral shape clearly intermediate

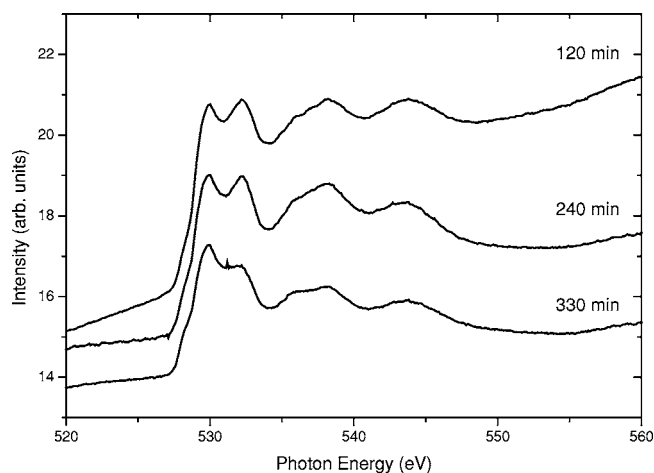


FIG. 5. Nanoparticles (9.7 nm) at the O K edges at an increasing Ar^+ etching time (500 eV). A vertical offset is used for clarity.

between the two cases. After 330 min of sputtering at low energy, as shown in Fig. 5, the proportion of the two components did not change substantially, acknowledging that, on the whole, the Ar^+ etching reduces the intensity of the O signal at the absorption edge. The *ex situ* prepared NPs have an “onion”-like structure, and our XAS experiments indicate that it is possible to remove the organic surfactant on the surface by means of Ar^+ ion etching at moderate energy without significantly affecting the NPs oxide shell. However, only by high Ar^+ etching energies (over 900 eV) and a long sputtering time was it possible to partially remove the metal oxide and to magnetize the NPs with a moderate magnetic field.

Finally, when the sample was further etched with Ar^+ at 1500 eV for 240 min and then at 3500 eV for a further 180 min, it was possible to record a small magnetic dichroic (XMCD) signal. After each sputtering step at 180, 240, and a final one after 300 min, all at 3500 eV, the sample was cooled to 15 K. During cooling, as before, a pulsed magnetic field of about 0.4 T was applied.

The upper panel of Fig. 6 shows the isotropic spectra for two etching times resulting from the sum of two subsequently measured spectra with reversed helicity ($\sigma^+ + \sigma^-$), taking into account the subtraction of the double step function (figure labels (a) and (b)). The corresponding XMCD signals ($\sigma^+ - \sigma^-$) are displayed in the lower panels. It is difficult to analyze the data of the Ar^+ etched samples in order to extract meaningful magnetic properties, mainly because it is extremely problematic to separate the metallic and nonmetallic contributions. The small signal recorded for these samples, essentially due to the measurements performed in remanence, leads to a significantly large error bar with deviations ranging from 5% to 10% of the values for the spin and orbital moments and up to 33% for the moments ratio.

The most relevant value that can be extracted from this data is the μ_l/μ_s^{eff} ratio, determined, according to the sum rules,^{12–14} directly using the ratio of the values of the integral calculated from the L_3 and L_2 edges. This value is independent from the geometrical conditions of the experiment and it has the advantage that it does not need an *a priori* knowledge

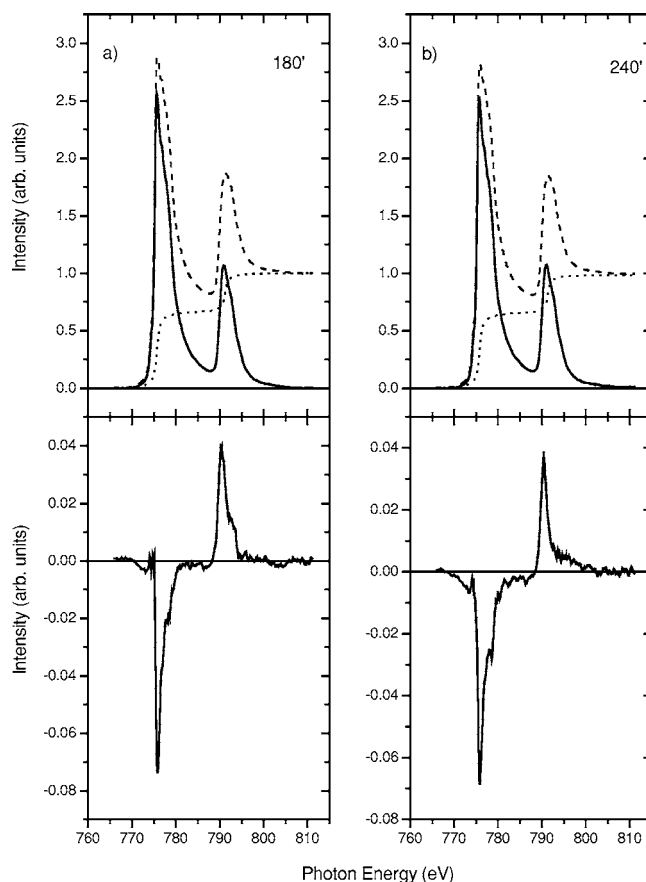


FIG. 6. Upper panel: dashed line, isotropic spectra ($\sigma^- + \sigma^+$); dotted line, step function; full line, isotropic spectrum minus step function. Lower panel: dichroism spectra ($\sigma^- - \sigma^+$) of an array of nanoparticles (9.7 nm) at Co $L_{3,2}$ edges after (a) 180 min and (b) 240 min Ar^+ etching (3.5 keV).

of the number of $3d$ holes in the ground state.¹² Furthermore, it allows us, in general, to safely compare values obtained under different measurement conditions. The contribution to the spin moment arising from the dipole interaction is neglected. The spin moment calculated applying the sum rules is then an effective value and it is labeled with “eff.”

A significant enhancement of the spin to orbital magnetic moment ratio, μ_l/μ_s^{eff} , with respect to bulk Co and in function of the Ar^+ etching time, can be observed. This behavior is in good agreement with the previously observed one for NPs of the same size measured also in remanent magnetization.⁷ The value of μ_l/μ_s^{eff} increases with the sputtering time from $\mu_l/\mu_s^{\text{eff}}=0.14$ after 180 min to $\mu_l/\mu_s^{\text{eff}}=0.18$ after 240 min.

A larger ratio $\mu_l/\mu_s^{\text{eff}}=0.3$, obtained after 300 min of high-energy (3500 eV) Ar^+ etching, was calculated using a dichroic spectrum of low quality. In such a case the application of the sum rules is difficult and leads to a large error of about 33% in the value. However, this high value for the orbital to spin moment is comparable to that reported in Ref. 7. High values of μ_l/μ_s^{eff} could be explained, considering the nature of the sputtered NPs and the investigating XAS technique. The electron mean free path is about 2 or 3 nm for both Co and CoO, making XMCD especially sensitive to the

surface and interface states.¹⁵ During the sputtering procedure the CoO thickness decreases considerably, then the relative weight of the Co core and of the Co/CoO interface increases in the detected intensity of the total electron yield. Since the surface roughness also increases, the broken or missing bonds connected with a strained surface considerably also increase. The value of $\mu_l/\mu_s^{\text{eff}}=0.24$ reported in Ref. 7 was measured after Ar⁺ etching of the sample for 135 min at 3 kV. The authors estimate that after this sputtering time a shell of CoO of about 2.5 nm still exists. In view of our observations it is not really surprising that by increasing energy and etching time the μ_l/μ_s^{eff} value increases further, while the oxide shell gets thinner, the surface gets rougher, and the number of crystal defects increases.

Another interesting aspect is the observation reported in Ref. 16 that sputtering a CoO single crystal creates Co metal islands on the crystal surface. Hence, we cannot also exclude, in our case, the partial formation of some double interfaces of Co/CoO/Co after hours of heavy argon ion etching. This could also contribute to the increased orbital to spin moment ratio. The geometrical and chemical definition of a NP surface is still uncertain after such heavy treatment.

The here-observed enhancement of the spin to orbital magnetic moment ratio μ_l/μ_s^{eff} , as a function of the Ar⁺ etching time, may be essentially attributed to an increase of the orbital magnetic moment μ_l , while the spin values μ_s^{eff} stay almost constant when considering the error bars. The surface and the Co/CoO interface of the NPs play a crucial role; they are the essential factor that enhances the orbital moment, as observed in our measurements. The disruption of the NPs surface by Ar⁺ etching lowers the surface symmetry and, consequently, leads to a reduced crystal field quenching of the orbital moment.¹⁷ Furthermore, at the surface of a strong ferromagnet like Co, the reduced coordination number leads to a decrease in the hybridization between *sp* and *d* states so that the number of majority *d* electrons increases. Since the charge neutrality must be respected, also the number of unoccupied minority *d* electrons increases. Therefore the exchange splitting and finally the magnetic moment tend to increase. The surface effects are also enhanced probably because of a decrease of the NPs diameter induced by the ion etching. All these factors, in principle, may explain qualitatively the enhanced orbital to spin magnetic moment ratio, μ_l/μ_s^{eff} and the enhanced orbital moment observed after the Ar⁺ sputtering procedure. The small dichroic signal found in the samples measured in remanent magnetization could be easily attributed to the fact that not all the NPs, except a small fraction, get oriented along the field direction during the cooling with a pulsed magnetic field applied at regular intervals.

B. H⁺ etching

Samples etched with hydrogen ions show a completely different behavior. Opposite to the Ar⁺ etched NPs, they do not have any dramatic increase of the moments ratio. With respect to argon, low-energy H⁺ etching (500 eV) seems to be extremely effective in reducing the CoO layer. The value of the ratio μ_l/μ_s^{eff} we calculated after 240 min of etching is

just slightly higher than for the Co bulk ($\mu_l/\mu_s^{\text{eff}}=0.095$ Ref. 14). As shown in Fig. 7(a), after only 120 minutes of etching at 500 eV, the typical edge splitting of the CoO is extremely reduced and the Co metallic character already prevails over the nonmetallic one. After 240 min of etching there is no more trace of CoO on the XAS signal. Considering that the technique is particularly sensitive to the surface and the μ_l/μ_s^{eff} ratio remains almost constant at about $\mu_l/\mu_s^{\text{eff}}=0.10$ and increases to $\mu_l/\mu_s^{\text{eff}}=0.12$ only after 240 min of H⁺ sputtering, we can conclude that the CoO shell was entirely reduced by means of the H⁺ etching procedure within a sputtering time that could be estimated between 180 and 240 min.

The quality of the dichroic signal shown in the low panels of Fig. 7 is much improved with respect to the one of Fig. 6. The dichroism, in this case, was calculated, subtracting two subsequent XAS scans measured, applying a constant 3 T magnetic field produced by superconductive coils and reversing its direction after each scan at room temperature. The quality of the dichroic signal increased enormously because the measurements in this case were performed in saturation with samples immersed in a high magnetic field. The high quality of the data, in contrast to the Ar⁺ etched samples, allows a more extensive analysis of the magnetic properties of the H⁺ reduced NPs.

The separate calculation of the orbital and spin moments is the nontrivial further step involved in the application of the sum rules. To obtain the two values μ_l and μ_s^{eff} it is necessary to subtract the contribution of the *s* states by means of a suitable double step function and to know the amount of 3*d* holes in the ground state.¹⁴ While the calculation of the step function for the L₃ and L₂ edges is almost straightforward and well established in the literature, the quantity of the 3*d* holes in the case of the NPs of our study cannot be easily calculated, in such a regard this point requires some caution. The NPs under study have mainly a crystallographic structure that includes fragments related to a multiple twisted fcc lattice¹ far from the regular structure of a well-ordered crystal. However, only for the sake of comparison of the μ_l and μ_s^{eff} values at a different etching time, we decided to use the n_{3d} value normally utilized for the Co bulk, $n_{3d}=7.5$.¹⁴ For this reason the given values of μ_l and μ_s^{eff} should be only applied in the context of this comparative study and are not intended to be absolute measured values for the chemically synthesized NPs.

The given values of the spin and orbital moments possess a systematic error that is difficult to evaluate. This systematic error becomes irrelevant only for the purposes of a relative comparison, on assuming that the n_{3d} value does not, or slowly, changes during sputtering. While the spectral curves of the Ar⁺ etched samples measured reversing the circular polarization, σ^+ and σ^- were corrected for a small offset before proceeding with their subtraction and the integral area calculation. No background corrections were necessary for the H⁺ sputtered samples. Self-absorption corrections were not considered, taking into account the nature of this comparative study and the large error connected with the inaccuracy of the measurements made in remanent magnetization on the Ar⁺-etched NPs.

The values of μ_l , μ_s^{eff} , and their ratio μ_l/μ_s^{eff} for the H⁺ sputtered samples are listed in Table I. In the case of

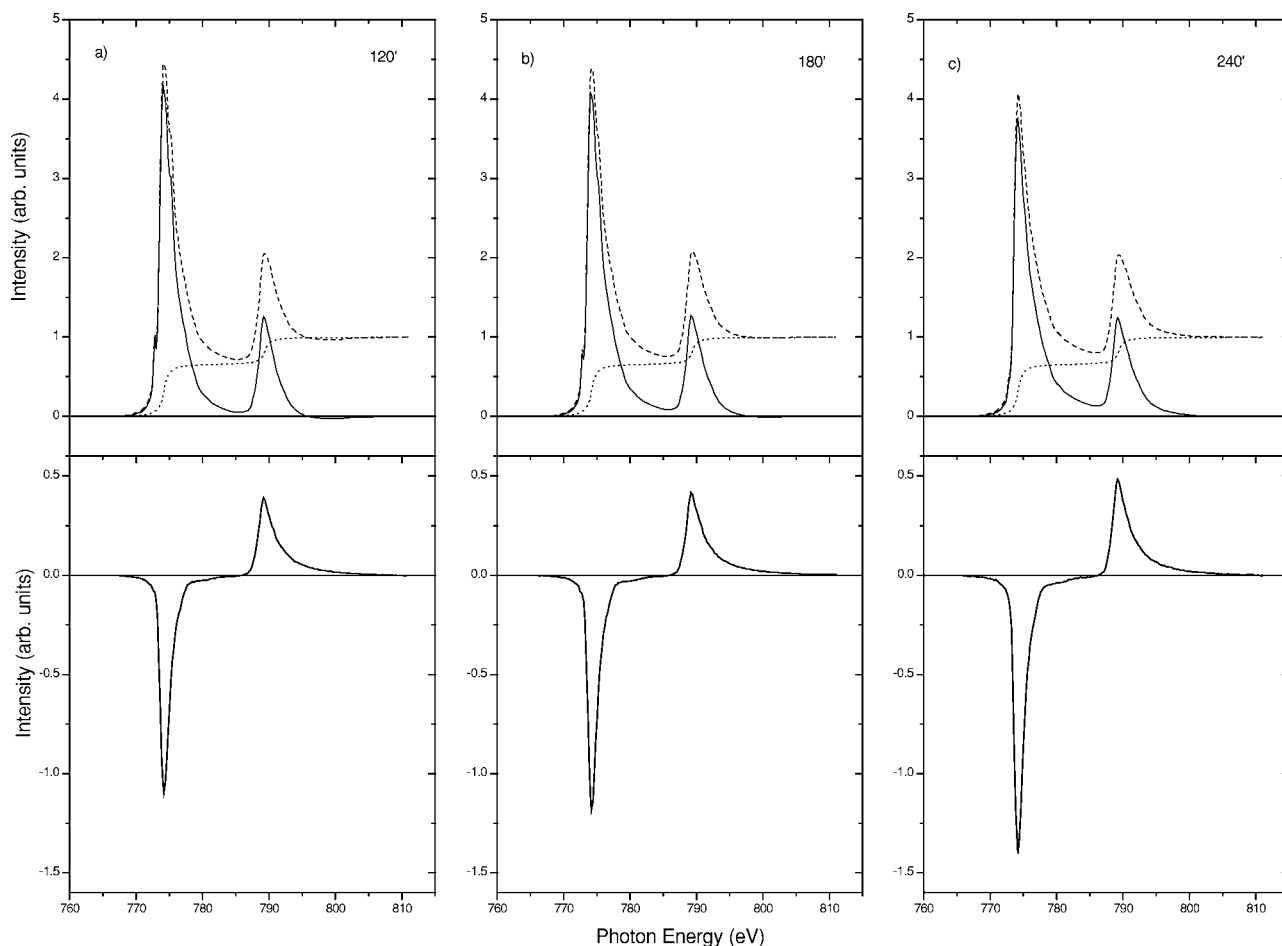


FIG. 7. Upper panel: dashed line, isotropic spectra; dotted line, step function; full line, isotropic spectrum minus step function. Lower panel: dichroism spectra of an array of nanoparticles (9.7 nm) at Co $L_{3,2}$ edges after (a) 120 min, (b) 180 min, and (c) 240 min H^+ etching (500 eV).

H^+ -etched samples the orbital moment remains stable between 120 and 180 min of sputtering and only after 240 min it reaches the value of $\mu_l=0.10(\mu_B/\text{atom})$. The spin moment increases constantly passing from $\mu_s^{\text{eff}}=0.67(\mu_B/\text{atom})$ after 120 minutes to $0.69(\mu_B/\text{atom})$ after 180 min and reach the value of $\mu_s^{\text{eff}}=0.79(\mu_B/\text{atom})$ after 180 min. As stressed before, these numbers are not important in their absolute value, but they give an idea of what effect the etching has on the sample surface.

C. H^+ and Ar^+ etching: A comparison

The orbital to spin moment ratio μ_l/μ_s^{eff} is independent of the method used to magnetize the NPs and allows us to

TABLE I. Orbital and spin magnetic moments of H^+ -etched Co nanoparticles.

H^+ -etching time (min)	μ_l (μ_B/atom)	μ_s^{eff} (μ_B/atom)	μ_l/μ_s^{eff}
120	0.07	0.67	0.10
180	0.07	0.69	0.10
240	0.10	0.79	0.12

directly compare the two sets of data obtained for the Ar^+ and the H^+ sputtered samples. With respect to Ar^+ , the H^+ sputtered samples show a dramatically different behavior. While for Ar^+ sputtered samples the estimated increase of the orbital magnetic moment can be easily attributed to the presence of a Co/CoO interface and to surface disruption, for the H^+ -etched samples an almost constant orbital moment points in the direction of a much less aggressive action of the H^+ etching on the NPs. The increased value of the μ_l/μ_s^{eff} ratio for the Ar^+ -etched samples can be substantially ascribed to a strong increase of the orbital moment while the spin moment, as already underlined, remains almost constant.

In the case of H^+ -etched samples, both orbital and spin magnetic moments increase their value as a function of the sputtering time. This fact points strongly to the increased μ_l/μ_s^{eff} ratio being caused by a residual presence of a Co/CoO interface as well as to a strained NPs surface caused by the heavy sputtering. In the case of the H^+ -etched samples there is an almost constant orbital to spin moment ratio that tends to increase only after a long sputtering time. This increase can then be attributed solely to the surface disruption, while the presence of a Co/CoO interface in this case after 240 min of H^+ ions etching can be excluded.

The effect of the light H⁺ ions is less devastating on the surface of the NPs than the heavy Ar⁺ bombardment, however, in this case the small increasing value of the ratio from $\mu_l/\mu_s^{\text{eff}}=0.10$ to $\mu_l/\mu_s^{\text{eff}}=0.12$, apart from the typical surface to bulk improved ratio for the NPs, could also be attributed to implanted H atoms in the Co NPs that distorts their already imperfect crystalline structure. As already underlined, the NPs prepared, following the synthetic route devised in Ref. 2, have a disordered crystal structure that is mainly comprised of fragments of a multiply twinned fcc structure. It is clear that changes in the crystalline structure, as, for example, an increase of the lattice constants determined by implanted H atoms, could give rise to slightly different values for the magnetic moment ratio. Given this, comparisons with NPs of different batches as well as prepared with different techniques or undergone to different chemical treatments must be considered very carefully. It is important to note that the numerical values of the spin and magnetic moments μ_l and μ_s^{eff} , obtained with the two different etching procedures, cannot be directly compared because of the different ways used to magnetize the samples and the probably different value of \mathbf{n}_{3d} due to the different etching procedures.

IV. CONCLUSION

We observed that low-energy Ar⁺ ion etching is an effective method in the removal of the organic coating on the

surface of the Co NPs. Long-time Ar⁺ sputtering at high energies induces a progressive and significant enhancement in the orbital to spin magnetic moment ratio, while low-energy and short-time H⁺ ion etching gives values of the moments ratio very similar to the bulk values of Co. We attributed the enhanced magnetic moment ratio seen in the Ar⁺ ion etched samples mainly to the Co/CoO interface and to the surface disruption of the NPs. The H⁺ ion etched samples appear to have the oxidized layers completely reduced and do not show an enhanced magnetic moment ratio. The calculated absolute values of the orbital and spin moments are subject to large errors, however, the pronounced development of their ratio as a function of the etching time gives valuable information on the effect of the Ar⁺ and H⁺ cleaning procedure of the *ex situ* prepared, chemically synthesized the NPs surface.

ACKNOWLEDGMENTS

We thank S. Rudorff for his invaluable technical support. We are also deeply indebted to Prof. A. Tennant, Dr. E. Gering, and Dr. K. Fauth for the stimulating scientific discussions and technical help.

-
- ¹C. B. Murray, Shouheng Sun, W. Gaschler, H. Doyle, T. A. Betley, and C. R. Kagan, *IBM J. Res. Dev.* **45**, 47 (2001).
²Dmitry P. Diniega and M. G. Bawendi, *Angew. Chem., Int. Ed.* **38**, 1788 (1999).
³S. Sun and C. B. Murray, *J. Appl. Phys.* **85**, 4325 (1999).
⁴M. Spasova, U. Wiedwald, R. Ramchal, M. Farle, M. Hilgendorff, and M. Giersig, *J. Magn. Magn. Mater.* **240**, 40 (2002).
⁵S. H. Baker, C. Binns, K. W. Edmonds, M. J. Maher, S. C. Thornton, S. Louch, and S. S. Dhesi, *J. Magn. Magn. Mater.* **247**, 19 (2002).
⁶M. Spasova and M. Farle, in *Low-Dimensional Systems: Theory, Preparation, and Some Applications*, NATO Science Serie II. Mathematics, Physics and Chemistry, edited by L. M. Liz-Marzán and M. Giersig, (Kluwer Academic, Netherlands, 2003), Vol. 91.
⁷U. Wiedwald, M. Spasova, E. L. Salabas, M. Ulmeanu, M. Farle, Z. Fraït, A. F. Rodriguez, D. Arvanitis, N. S. Sobal, M. Hilgendorff, and M. Giersig, *Phys. Rev. B* **68**, 064424 (2003).
⁸L. Soriano, M. Abbate, A. Fernández, A. R. González-Elipse, F. Sirotti, and J. M. Sanz, *J. Phys. Chem. B* **103**, 6676 (1999).
⁹J. B. Kortright, D. D. Awschalom, J. Stöhr, S. D. Bader, Y. U. Idzerda, S. S. P. Parkin, Ivan K. Schuller, and H.-C. Siegmann, *J. Magn. Magn. Mater.* **207**, 7 (1999).
¹⁰C. B. Murray, S. Sun, H. Doyle, and T. Betley, *MRS Bull.* **26**, 985 (2001).
¹¹U. Englisch, H. Rossner, H. Maletta, J. Bahrtdt, S. Sasaki, F. Senf, K. J. S. Sawhney, and W. Gudat, *Nucl. Instrum. Methods Phys. Res. A* **467–468**, 541 (2001).
¹²B. T. Thole, P. Carra, F. Sette, and G. van der Laan, *Phys. Rev. Lett.* **68**, 1943 (1992).
¹³P. Carra, B. T. Thole, M. Altarelli, and Xindong Wang, *Phys. Rev. Lett.* **70**, 694 (1993).
¹⁴C. T. Chen, Y. U. Idzerda, H.-J. Lin, N. V. Smith, G. Meigs, E. Chaban, G. H. Ho, E. Pellegrin, and F. Sette, *Phys. Rev. Lett.* **75**, 152 (1995).
¹⁵T. J. Regan, H. Ohldag, C. Stamm, F. Nolting, J. Lüning, J. Stöhr, and R. L. White, *Phys. Rev. B* **64**, 214422 (2001).
¹⁶C. Mocuta, A. Barbier, and G. Renaud, *Appl. Surf. Sci.* **162–163**, 56 (2000).
¹⁷M. Tischer, O. Hjortstam, D. Arvanitis, J. H. Dunn, F. May, K. Baberschke, J. Trygg, J. M. Wills, B. Johansson, and O. Eriksson, *Phys. Rev. Lett.* **75**, 1602 (1995).